

Low-dissipation data bus via coherent quantum dynamicsDylan Lewis ^{1,*}, João P. Moutinho,^{2,3} Antonio T. Costa,⁴ Yasser Omar ^{2,5,6} and Sougato Bose¹¹*Department of Physics and Astronomy, University College London, London WC1E 6BT, United Kingdom*²*Instituto Superior Técnico, Universidade de Lisboa, 1049-001 Lisbon, Portugal*³*Instituto de Telecomunicações, 1049-001 Lisbon, Portugal*⁴*International Iberian Nanotechnology Laboratory, 4715-330 Braga, Portugal*⁵*Centro de Física e Engenharia de Materiais Avançados (CeFEMA),
Physics of Information and Quantum Technologies Group, 1049-001 Lisbon, Portugal*⁶*PQI – Portuguese Quantum Institute, 1600-531 Lisbon, Portugal*

(Received 10 May 2023; revised 19 July 2023; accepted 21 July 2023; published 9 August 2023)

The transfer of information between two physical locations is an essential component of both classical and quantum computing. In quantum computing the transfer of information must be coherent to preserve quantum states and hence the quantum information. We establish a simple protocol for transferring one- and two-electron encoded logical qubits in quantum dot arrays. The theoretical energetic cost of this protocol is calculated—in particular, the cost of freezing and unfreezing tunneling between quantum dots. Our results are compared with the energetic cost of shuttling qubits in quantum dot arrays and transferring classical information using classical information buses. Only our protocol can manage constant dissipation for any chain length. This protocol could reduce the cooling requirements and constraints on scalable architectures for quantum dot quantum computers.

DOI: [10.1103/PhysRevB.108.075405](https://doi.org/10.1103/PhysRevB.108.075405)**I. INTRODUCTION**

Quantum dot quantum computers encode qubit states using electrons isolated in confined regions by electric fields. Efficiently transferring qubit states in these semiconductor-based architectures is a significant unresolved problem for their scalability. Recent proposals have focused on coherently shuttling the electrons [1,2] and on transfer through multiple quantum dots using engineered tunnel couplings [3], which employs theoretical results from work in perfect state transfer [4–6].

A distinct but related question is the energetic cost of using electric currents for the transfer of information in semiconductor-based classical computation. Generating the required potential gradients is a major source of energetic cost.

Landauer's principle states that the energy dissipated in the form of heat to erase a bit of information is $k_B T \log 2$ [7], suggesting a minimum energetic cost for computation. However, any computation can be performed reversibly [8], and the Landauer limit can in theory be surpassed. Despite further work on computing using reversible logic [9], there remain essentially no practical implementations that are both frictionless and fast. Adiabatic computing, which is slow reversible computing, has been proposed but with significant

reductions in performance [10,11]. Quantum computing, using unitary evolutions, is inherently reversible and therefore provides a possible platform for low-energy computation. The coherent manipulation of single electrons for classical computation has recently been proposed, with Moutinho *et al.* [12] considering the energetic advantage of using a quantum dot array with Fredkin gates to implement a full adder, raising the pertinent question of whether a classical computer based on the use of small quantum systems could provide an energetic advantage for classical computation. The logical states of the qubits are one- and two-electron encodings. Motivated by this, we address the question of low-dissipation quantum buses in quantum dot architectures for quantum and classical data. In this model of a quantum data bus, linear chains of qubits can effectively transfer quantum information via the natural evolution of an interacting Hamiltonian. In theory, quantum state transfer [4,5] can coherently transfer information via quantum states without necessarily requiring a voltage.

Currently, computers are many orders of magnitude from the Landauer limit, with the most powerful supercomputers consuming on the order of keV to MeV per bit operation [12]. Despite the effort in reducing computational energetic costs, the fundamental limits for electron-based computing suggest that the interconnects—fixed wiring—are the *primary* factor limiting the efficiency of computation, potentially orders of magnitude more costly than the computation itself [13]. Here we address this problem directly by proposing a classical bus using coherent quantum dynamics where the energetic cost does not scale with the length of the wire. We establish a protocol for efficient transfer of an electron using perfect state transfer chains and a simple electron separation protocol. This protocol could be used for quantum computation to alleviate

*dylan.lewis.19@ucl.ac.uk

some cooling constraints in scalable quantum computing architectures [14]. We find the energetic cost of changing the tunnel coupling between two quantum dots and the minimum energetic cost of implementing the protocol. This is compared to our computed minimum energetic costs for shuttling and for classical data buses. We also make a note on the effect of noise in experimental quantum dot arrays.

II. PHYSICAL MODEL

For the quantum dot chains that we consider, the logical qubit is encoded in the charge, rather than the spin. The state transfer is a state $|\psi_1(t_0)\rangle$ at time t_0 , initialized on quantum dot 1 in the chain, being transferred to the last quantum dot in the chain at specific time T , $|\psi_N(T)\rangle$, with a high fidelity, $F = |\langle\psi_1(t_0)|\psi_N(T)\rangle|^2$.

We set the initial time $t_0 = 0$ and the initial state for transfer to $|\psi(0)\rangle = |\psi_1(0)\rangle \otimes |0\rangle \otimes \dots \otimes |0\rangle$. The protocol, in the simplest case, involves simply turning on the interactions for a specific time T and then turning off the interactions. The state is then at the final site N with high fidelity.

A. Hubbard model

The general model for interacting quantum dots is an extended Hubbard Hamiltonian with both capacitive and tunnel coupling,

$$\begin{aligned} \frac{H}{\hbar} = & \sum_{i,\sigma} \varepsilon_i \hat{n}_{i,\sigma} + \sum_{i,\sigma} \Gamma_i (c_{i,\sigma}^\dagger c_{i+1,\sigma} + c_{i+1,\sigma}^\dagger c_{i,\sigma}) \\ & + \sum_{i,\sigma,\sigma'} V_i \hat{n}_{i,\sigma} \hat{n}_{i+1,\sigma'} + \sum_i U_i \hat{n}_{i,\uparrow} \hat{n}_{i,\downarrow}, \end{aligned} \quad (1)$$

where ε_i is the local field applied to quantum dot i , Γ_i is the tunnel coupling between quantum dots i and $i+1$, V_i is the capacitive coupling between quantum dots i and $i+1$, U_i is the onsite interaction at site i , and $c_{i,\sigma}$ and $c_{i,\sigma}^\dagger$ are the annihilation and creation operators, respectively, of an electron on quantum dot i with spin σ . The number operator for electrons of spin σ is therefore $\hat{n}_{i,\sigma} = c_{i,\sigma}^\dagger c_{i,\sigma}$.

B. Simplified models

In the transfer protocol, we start with an initial state that contains either one or two electrons, depending on the logical encoding used. Hence, assuming the spins of the electrons do not flip and the number of electrons is constant, significant simplifications to the general Hubbard model can be made. For a single-electron logical qubit, we simply have the tunnel-coupling term and local potential,

$$\frac{H_1}{\hbar} = \sum_{i=1}^{N-1} \Gamma_{i,i+1} (|i\rangle\langle i+1| + \text{H.c.}) + \sum_{i=1}^{N-1} \varepsilon_i |i\rangle\langle i|, \quad (2)$$

where we have defined a single-electron basis for the quantum dot chain: $|i\rangle$ indicates an electron at quantum dot i with the rest of the dots in the chain empty. The spin of the electron is assumed to be unchanged throughout the protocol. The model is more complex for the two-electron encoding. We introduce a two-electron state $|i, j\rangle$, with a spin-up electron at site i and a spin-down electron at site j . There are N sites in the set S .

The basis can therefore be labeled by $p \in S \times S = \{(i, j) | i \in S \text{ and } j \in S\}$, giving length N^2 , and can be constructed as $|p\rangle = |i, j\rangle = c_{i,\uparrow}^\dagger c_{j,\downarrow}^\dagger |0\rangle$. The Hamiltonian matrix elements are thus

$$H_{p,p'} = \langle 0 | c_{j,\downarrow} c_{i,\uparrow} H c_{i',\uparrow}^\dagger c_{j',\downarrow}^\dagger | 0 \rangle. \quad (3)$$

The anticommutation relations of fermions must be considered, $\{c_{i,\sigma}, c_{j,\sigma'}\} = \{c_{i,\sigma}^\dagger, c_{j,\sigma'}^\dagger\} = 0$ and $\{c_{i,\sigma}, c_{j,\sigma'}^\dagger\} = \delta_{i,j} \delta_{\sigma,\sigma'}$. With this careful choice of basis, such that the order of creation operators for the up spin and down spin are not permuted, we find

$$\begin{aligned} \frac{H_2}{\hbar} = & \sum_{i,j=1}^{N-1} [\Gamma_{i,i+1} (|i, j\rangle\langle i+1, j| + \text{H.c.}) \\ & + \Gamma_{j,j+1} (|i, j\rangle\langle i, j+1| + \text{H.c.}) \\ & + U \delta_{i,j} |i, j\rangle\langle i, j| \\ & + V (\delta_{i,j+1} + \delta_{i+1,j}) |i, j\rangle\langle i, j| \\ & + (\varepsilon_i + \varepsilon_j) |i, j\rangle\langle i, j|], \end{aligned} \quad (4)$$

where $\delta_{i,j}$ is the Kronecker delta, and we have assumed the onsite interaction U and capacitive coupling V are the same for all quantum dots. These Hamiltonians live in significantly smaller Hilbert spaces than the full Hubbard model, which is a space that increases exponentially with the number of quantum dots N . On the other hand, for $H_1 \in \mathcal{H}_1$ and $H_2 \in \mathcal{H}_2$, we have $\dim(\mathcal{H}_1) \sim N$ and $\dim(\mathcal{H}_2) \sim N^2$, which are both significantly simpler to simulate.

III. STATE TRANSFER WITH A SINGLE ELECTRON

The single-electron Hamiltonian of Eq. (2) is equivalent to the Hamiltonian of the single-excitation subspace dynamics of the XY model—a well-studied model for state transfer [6]. We consider schemes that limit the use of local fields, described by strength ε_i at site i , because additional local fields would increase the engineering complexity. The energetic costs of both this protocol and of a classical information bus are addressed in Sec. V.

In fact, perfect state transfer can be achieved directly with the XY model in a number of ways that do not require local fields. Engineering the spin-chain tunnel couplings can lead to perfect state transfer. This can be seen by rewriting Eq. (2) in matrix form,

$$\frac{H_1}{\hbar} = \begin{pmatrix} \varepsilon_1 & \Gamma_{1,2} & 0 & \dots & & \\ \Gamma_{1,2} & \varepsilon_2 & \Gamma_{2,3} & 0 & \dots & \\ 0 & \Gamma_{2,3} & \varepsilon_3 & \Gamma_{3,4} & 0 & \dots \\ \vdots & 0 & \Gamma_{3,4} & \varepsilon_4 & \Gamma_{4,5} & \dots \\ \vdots & \vdots & \vdots & \vdots & \vdots & \ddots \end{pmatrix}. \quad (5)$$

First, note that the raising and lowering operators of a large spin with $s = (N-1)/2$ act on basis states as $\hat{S}_\pm |s, m\rangle = \sqrt{s(s+1) - m(m \pm 1)} |s, m \pm 1\rangle$. For given s and quantum dot $1 \leq i \leq N$, we find $m = i - 1 - s$. Rotations of the spin can be induced by S_x , which is the generator of rotations about the x axis in $SO(3)$, giving $R_x(\theta) = e^{-iS_x \theta}$. With the relationships above, we see that H_1 is equivalent to $2S_x = S_+ + S_-$ by

setting $\varepsilon_i = 0$ for all i and

$$\begin{aligned}\Gamma_{i,i+1} &= \sqrt{s(s+1) - m(m+1)} \\ &= \sqrt{i(N-i)}.\end{aligned}\quad (6)$$

After a time $T = \pi/2$, which gives unitary evolution $U(\pi/2) = e^{-iH_1\pi/2\hbar} = e^{-iS_x\pi}$, a rotation of π around the x axis has been induced. This takes the initial state $|1\rangle$ to the final state $|N\rangle$, thus performing perfect state transfer in time $T \sim N$, where the tunnel coupling has been scaled such that the largest coupling is 1.

We can also use the superexchange where the two end qubits are weakly coupled to a relatively strongly coupled many-body quantum system [15–18]. In this case the many-body quantum system is the central quantum dots of the chain. While the fidelity of state transfer is high, the superexchange is very slow: if the coupling between the central quantum dots is such that $\Gamma_{i,i+1} \sim 1$, and the coupling of the first and final quantum dots to the central chain is $\Gamma_{1,2} = \Gamma_{N-1,N} = \epsilon$, where $\epsilon \ll 1$, then the transfer time is $T \sim 1/\epsilon^2$. Slow transfer is undesirable for scalable and fast computational architectures because it requires a slow clock frequency.

IV. STATE TRANSFER WITH TWO ELECTRONS

State transfer for two electrons is less straightforward. Although too slow for an architecture proposal, we note that transfer using the superexchange is still possible with two electrons.

Realizing perfect state transfer in the same way as the single-electron case, with engineered spin chains replicating S_x for a large spin s , is not possible for nonzero U and V because all diagonal terms would have to be constant (or zero). In the case of two electrons, we would require

$$U\delta_{i,j} + V(\delta_{i,j+1} + \delta_{i+1,j}) + \varepsilon_i + \varepsilon_j = d, \quad (7)$$

for all i and j . If we consider $|i-j| > 1$, ε_i must be the same for all i . Thus $U = V = 0$ is required for all diagonal elements to be equal. In this case we could then use the same tunnel couplings as the single-electron case and have two noninteracting electrons that both separately perform perfect state transfer at the same time. If $U \ll \Gamma_{\min}$, where Γ_{\min} is the smallest coupling $\Gamma_{1,2}$, we have pretty good (not perfect) state transfer—which, given that this work is also motivated by low-dissipation classical computing, would be useful if it is experimentally feasible. For example, a chain of 16 quantum dots, with $U = \Gamma_{\min}/10$, has a fidelity of state transfer of greater than 0.9.

We propose a protocol that first involves separating the electrons and then transferring one electron at a time along an engineered chain with perfect state transfer before recombination.

Two electrons and two quantum dots

The dynamics of two electrons with two quantum dots can be tuned such that there is high fidelity of electron separation, so one electron on each dot. Perfect state transfer could occur with two electrons on two quantum dots if the Hamiltonian for the evolution of the states—the adjacency matrix of the graph

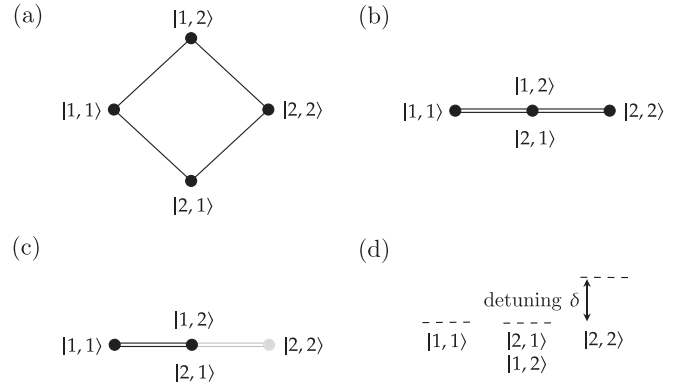


FIG. 1. Graphs of states in various representations: (a) all two-electron two-quantum-dot states are considered where the electrons have opposite spins, (b) simplification of the graph due to symmetry and initial states; and (c) state $|2, 2\rangle$ is suppressed due to detuning represented in (d).

with additional diagonal terms—can be written as

$$\frac{H}{\hbar} = \Gamma \begin{pmatrix} 0 & 1 & 1 & 0 \\ 1 & 0 & 0 & 1 \\ 1 & 0 & 0 & 1 \\ 0 & 1 & 1 & 0 \end{pmatrix} + d\mathbb{1}, \quad (8)$$

where d would have no effect on the evolution, see Fig. 1(a) for the graph. The analysis can be simplified for certain initial states. The states $|1, 2\rangle$ and $|2, 1\rangle$ can be considered together because the quantum walk evolution, $U = e^{-iHt/\hbar}$, is symmetric with respect to these states if we start from $|1, 1\rangle$ or $|2, 2\rangle$, see Fig. 1(b). This gives the adjacency matrix

$$A = \sqrt{2}\Gamma\hbar \begin{pmatrix} 0 & 1 & 0 \\ 1 & 0 & 1 \\ 0 & 1 & 0 \end{pmatrix}, \quad (9)$$

which is equal to $2\Gamma S_x$, where S_x is the spin operator along the x direction for an $s = 1$ boson. Thus, if we assume no detuning between sites, A is equivalent to a rotation around the x axis and, as before, perfect state transfer occurs in time $T = \pi\hbar/2\Gamma$.

If we detune the final state $|2, 2\rangle$ from the rest, we suppress the coherent transfer to this site. The dynamics now lead to a high fidelity transfer between $|1, 1\rangle$ and a superposition of $|1, 2\rangle$ and $|2, 1\rangle$, precisely the state required for coherent electron separation. To demonstrate the cause of the suppression, consider only the interaction of the superposition of the separated electrons with the $|2, 2\rangle$ state, so a two-state system with one of the states detuned by δ . Relabeling the basis states $|0\rangle$ and $|1\rangle$, we have the Hamiltonian

$$\frac{H}{\hbar} = \Gamma\sigma_x - \frac{\delta}{2}\sigma_z + \frac{\delta}{2}\mathbb{1}, \quad (10)$$

where σ_x and σ_z are the standard Pauli matrices. We can neglect the identity term as it only adds a global phase. The evolution of the state is therefore

$$\begin{aligned}U(t) &= e^{-i(\Gamma\sigma_x - \frac{\delta}{2}\sigma_z)t} \\ &= \cos(nt)\mathbb{1} + i\frac{\delta}{2n}\sin(nt)\sigma_z - i\frac{\Gamma}{n}\sin(nt)\sigma_x,\end{aligned}\quad (11)$$

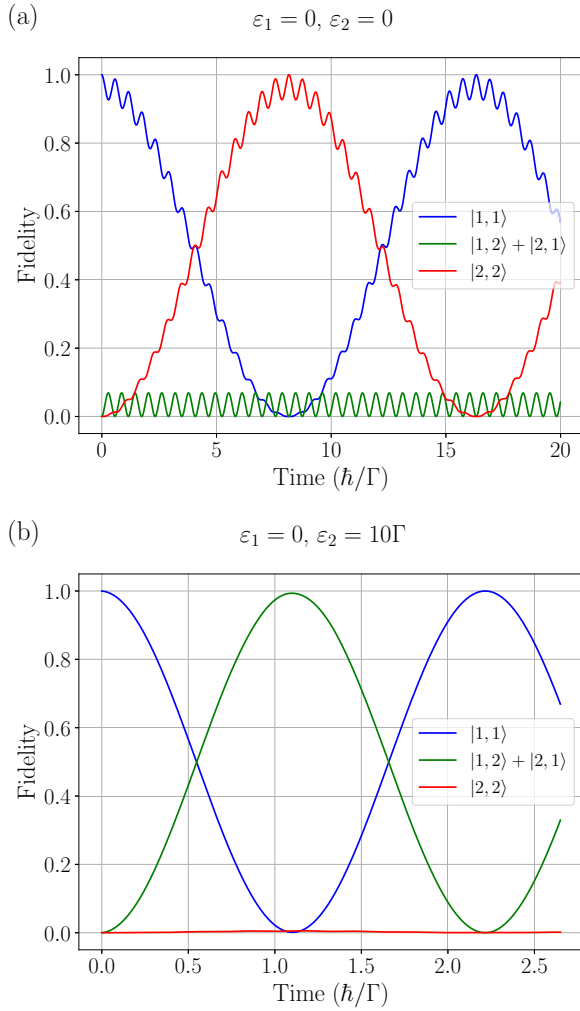


FIG. 2. Comparison of the fidelity for the separation of the electrons with $U = 20\Gamma$, $V = 10\Gamma$ (Γ is tunnel coupling) for (a) no local fields, showing the electrons essentially remain bound together, and (b) $\varepsilon_2 = 10\Gamma$, showing a maximum electron separation fidelity of 0.993.

where $n = \sqrt{\Gamma^2 + (\delta/2)^2}$. When $\delta = m\Gamma$ with m an integer larger than 1, the σ_x term is suppressed by $1/\sqrt{1 + \frac{m^2}{4}}$. For $m \gg 1$ we have a suppression of $\sim 2/m$ for the rotation term. This leads to a reduction in the fidelity of oscillations from $|0\rangle$ to $|1\rangle$ by approximately $4/m^2$.

Typical values for electron interaction and capacitive coupling are $U = 20\Gamma$ and $V = 10\Gamma$, where Γ is the tunnel coupling between the two quantum dots [19,20]. Applying a local field $\varepsilon_2 = 10\Gamma$ to only the second quantum dot detunes the state $|2, 2\rangle$ by $\delta = 20\Gamma$, while the energy of the states $|1, 1\rangle$, $|1, 2\rangle$, and $|2, 1\rangle$ are all equal. Using the analysis above, we should therefore find a reduction of the fidelity, leading to the $|2, 2\rangle$ state of approximately 0.01. Numerically, we find a maximum fidelity of separation for the electrons of 0.993, see Fig. 2. The fidelity can be made higher if we use quantum dots with no capacitive coupling, so $V = 0$, and a local field $\varepsilon_2 = 20\Gamma$, which keeps the energy of the other states equal. The detuning is now $\delta = 40\Gamma$, giving an analytical fidelity loss of approximately 0.0025, which is very close to what

we find numerically: A fidelity of separation of 0.998. The time for the electron separation is that of oscillations in a two-state system with interaction strength $\sqrt{2}\Gamma$ —the factor of $\sqrt{2}$ is because there are actually two states $|1, 2\rangle$ and $|2, 1\rangle$ and therefore two paths between $|1, 1\rangle$ to the other node of the effective graph. Electron separation therefore occurs in time $T = \pi\hbar/2\sqrt{2}\Gamma$, which is what we find numerically.

For general U and V , to keep the energy of states $|1, 1\rangle$, $|1, 2\rangle$, and $|2, 1\rangle$ equal we set $\varepsilon_2 = \varepsilon_1 + U - V$, giving the detuning $\delta = 2\varepsilon_2 - 2\varepsilon_1$. The larger U is, while minimizing V , the larger the difference between ε_2 and ε_1 , which increases δ and therefore the fidelity of electron separation.

Once the electrons have been separated they are coherently transferred sequentially along the central spin chain with engineered couplings, as in the single-electron case. In theory, this step gives unit fidelity for state transfer. Noise is discussed in Sec. VI. The electrons are then recombined using the inverse of the separation procedure, with essentially the same fidelity. Figure 3 shows the steps of the protocol.

V. ENERGETIC COST

The energetic cost of both the single- and two-electron quantum buses are now considered. As a benchmark we compare the energetic cost of shuttling electrons and the lower bound of a data bus in a classical CPU.

With engineered couplings, the transfer of the electron is coherent. Hence the transfer itself does not require an energy source—the reason for an energetic advantage. However, the interactions must be turned on and off, which does have an energetic cost. The local fields do not require turning on and off and therefore do not have an energetic cost associated with each transfer.

A. Energetic cost of freezing and unfreezing interactions

We show that freezing and unfreezing the interactions for a quantum dot system has an optimal energetic cost equivalent to approximately the charging energy of a quantum dot, E_C . The energetic cost of freezing and unfreezing interactions can be estimated by considering a double quantum dot with two electrons.

There are two limiting cases: The barrier potential going to zero giving one large quantum dot with two electrons, and the barrier potential being very high giving two isolated quantum dots each with harmonic potential. In our quantum dot model, we consider the latter case, with a significant barrier. This assumption is reasonable since the preceding protocol for state transfer is in the regime $U \gg \Gamma$.

Electrons in a double quantum dot can be modeled as a biquadratic potential [19,21–24], see Fig. 4. The Hamiltonian for two electrons is

$$H = \sum_{j=1}^2 \left[\frac{\mathbf{p}_j^2}{2m^*} + V(\mathbf{r}_j) \right] + \frac{e^2}{4\pi\epsilon_0\epsilon_r} \frac{1}{|\mathbf{r}_1 - \mathbf{r}_2|}, \quad (12)$$

where \mathbf{p}_j and \mathbf{r}_j are the momentum and position vectors of electron j in two dimensions, m^* is the effective mass, and

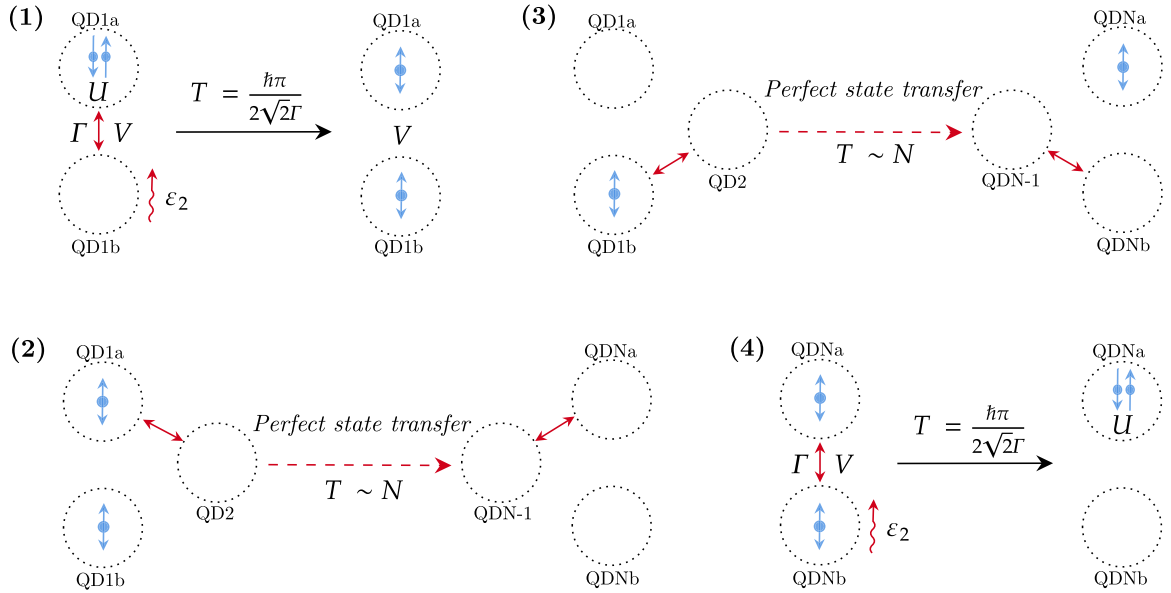


FIG. 3. Energy-efficient protocol for transfer of a two-electron logical qubit (or bit) has four steps: (1) the initial state is loaded into quantum dot 1a (QD1a), and split into an equal superposition of both spins in QD1a and QD1b using electron separation protocol; (2) and (3) perfect state transfer is used to transfer each electron individually; and (4) the electrons are recombined onto QDNa.

$V(\mathbf{r})$ is the potential

$$V(\mathbf{r}) = V_0 \min[(\mathbf{r} - \mathbf{l})^2, (\mathbf{r} + \mathbf{l})^2, \mu], \quad (13)$$

where μ is the chemical potential, and the dots are located at $\pm \mathbf{l}$, a distance of $d = 2l$ apart. For large μ , we consider the simplification $V_S(\mathbf{r}) = \lim_{\mu \rightarrow \infty} V(\mathbf{r})$. Figure 4 shows the form of the potential, with barrier height $V_B = V_0 l^2$ between the dots. Increasing the distance between the harmonic potentials increases the barrier height. Rather than increasing the distance, however, d is fixed and the strength of the harmonic potentials V_0 is increased. In the low-temperature limit, $k_B T \ll \hbar \omega_0$, the electrons are assumed to be in their ground state. For a two-dimensional harmonic trap with $V_0 = m^* \omega_0^2 / 2$, the ground-state energy, with lowest orbital momentum in the confinement, is $\hbar \omega_0$. We define a dimensionless parameter $\eta = m^* \omega_0 l^2 / \hbar$, which is the ratio of the barrier height and half the ground-state energy of an electron in a harmonic trap. In this analysis, only $\eta > 1$ is considered, following from $U \gg \Gamma$. In this regime, the Heitler-London (HL)

approximation is valid [24], since the quantum dots are sufficiently separated. We can thus build the two-electron ground state from single-electron harmonic ground states of model Hamiltonians of the form $h_{L/R}^{(0)} = \mathbf{p}_{L/R}^2 / 2m^* + m^* \omega_0^2 (\mathbf{r}_1 \pm \mathbf{l})^2 / 2$.

If there are no external fields, the ground state of two electrons will always be the singlet state because the spatial wave function is symmetric, i.e., exchange coupling $J \equiv E_T - E_S > 0$ [23], where $E_{T/S}$ are the triplet and singlet energies. Furthermore, we will consider two electrons on the same quantum dot to calculate the charging energy E_C . The lowest energy is when both electrons can occupy the same lowest energy orbital, giving a symmetric spatial wave function, and therefore a singlet spin state. As we are not concerned with the exchange coupling, we only consider the singlet state in the following HL approximation and further analysis.

The ground state of the harmonic potentials for the left and right quantum dots, with Hamiltonians $h_{L/R}^{(0)}$, is

$$\varphi_{L/R}(\mathbf{r}) = \langle \mathbf{r} | L/R \rangle = \frac{1}{a\sqrt{\pi}} e^{-\frac{1}{2a^2} [(x \pm l)^2 + y^2]}, \quad (14)$$

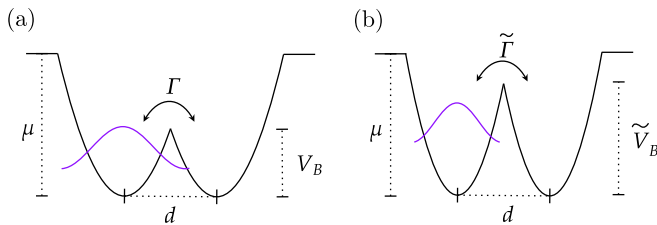


FIG. 4. One-dimensional cross section through the center of the confining harmonic potentials that model a double quantum dot. The confinement is in two dimensions, with radial symmetry around the center of each of the dots. The size of V_0 has been changed between (a) and (b), with (b) showing increased confinement and therefore a higher barrier.

where we have defined a Bohr radius $a = \sqrt{\hbar / m^* \omega_0}$, $\mathbf{r} = (x, y)$, and the dots are centered along the x axis. Using the HL approximation, the ground state of the two-electron double quantum dot is a symmetric spatial superposition of the electrons on different dots. We define the overlap between the adjacent harmonic potentials, $s = \langle L | R \rangle = e^{-l^2/a^2} = e^{-\eta}$. As in Ref. [25], the Hund-Mulliken (HM) approximation is used to further include the states with two electrons on the same quantum dot, the (2,0) and (0,2) states, which must also be singlet states in the ground state. The left and right basis states are rotated such that they are orthogonal, $\langle \Phi_L | \Phi_R \rangle = 0$, giving $|\Phi_{L/R}\rangle = (|L/R\rangle - g|R/L\rangle) / \mathcal{N}$, where $\mathcal{N} = \sqrt{1 - 2sg + g^2}$ and $g = (1 - \sqrt{1 - s^2}) / s$, such that both \mathcal{N} and g are

functions of η . In this basis, with $\Phi_{L/R}(\mathbf{r}) = \langle \mathbf{r} | \Phi_{L/R} \rangle$, the three relevant spatial wave functions are

$$\Psi_L^d(\mathbf{r}_1, \mathbf{r}_2) = \Phi_L(\mathbf{r}_1)\Phi_L(\mathbf{r}_2), \quad (15)$$

$$\Psi_R^d(\mathbf{r}_1, \mathbf{r}_2) = \Phi_R(\mathbf{r}_1)\Phi_R(\mathbf{r}_2), \quad (16)$$

$$\Psi_0^s(\mathbf{r}_1, \mathbf{r}_2) = \frac{1}{\sqrt{2}}[\Phi_L(\mathbf{r}_1)\Phi_R(\mathbf{r}_2) + \Phi_R(\mathbf{r}_1)\Phi_L(\mathbf{r}_2)], \quad (17)$$

where $\Psi_{L/R}^d(\mathbf{r}_1, \mathbf{r}_2)$ indicate the doubly occupied states (2,0) and (0,2), and $\Psi_0^s(\mathbf{r}_1, \mathbf{r}_2)$ indicates both sites being singly occupied (1,1). All these states are symmetric since the states are spin singlets.

The Hamiltonian is separable for the non-Coulomb terms: $\hat{H} = \hat{h} \otimes \mathbb{1} + \mathbb{1} \otimes \hat{h} + \hat{C}$, where $\hat{h} = \mathbf{p}^2/2m^* + V_S(\mathbf{r})$, and $\hat{C} = e^2/4\pi\epsilon_r\epsilon_0|\mathbf{r}_1 - \mathbf{r}_2|$. The tunneling terms, from the states $\Psi_L^d(\mathbf{r}_1, \mathbf{r}_2)$ or $\Psi_R^d(\mathbf{r}_1, \mathbf{r}_2)$ to $\Psi_0^s(\mathbf{r}_1, \mathbf{r}_2)$, are then given by the matrix element

$$\hbar\Gamma^{(2)} = \sqrt{2}\langle \Phi_{L/R} | \hat{h} | \Phi_{R/L} \rangle + \langle \Psi_{L/R}^d | \hat{C} | \Psi_0^s \rangle, \quad (18)$$

where we have defined a two-electron tunneling rate $\Gamma^{(2)}$, including the Coulomb repulsion. If there is no Coulomb repulsion and we ignore the presence of the second electron, we have the ‘‘bare’’ tunneling rate,

$$\begin{aligned} \hbar\Gamma &= \langle \Phi_{L/R} | \hat{h} | \Phi_{R/L} \rangle, \\ &= \frac{1}{\sqrt{2}}[(1 + g^2)w - 2gu], \end{aligned} \quad (19)$$

where we have used $w = \langle L | \hat{h} | R \rangle = \langle R | \hat{h} | L \rangle$ and $u = \langle L | \hat{h} | L \rangle = \langle R | \hat{h} | R \rangle$. Furthermore, we find

$$w = \left(1 - \sqrt{\frac{\eta}{\pi}}\right)e^{-\eta}\hbar\omega_0 \quad (20)$$

and

$$u = \left(1 - \sqrt{\frac{\eta}{\pi}}e^{-\eta} + \eta \operatorname{erfc}(\sqrt{\eta})\right)\hbar\omega_0, \quad (21)$$

where $\operatorname{erfc}(\sqrt{\eta})$ is the complementary error function.

The charging energy E_C is approximately the difference in energy between having two electrons in the lowest energy level of a single quantum dot and having only one electron in the dot,

$$E_C \approx E_0^{(2)} - E_0^{(1)}, \quad (22)$$

where $E_0^{(1)}$ ($E_0^{(2)}$) is the ground-state energy of 1 (2) electrons in a single harmonic potential. For a single electron in a harmonic trap, as above, $E_0^{(1)} = \hbar\omega_0$. The two-electron case in a single harmonic potential is more complex, since the Coulomb repulsion of the two electrons must be considered, and in the double-quantum-dot model above, we have

$$\begin{aligned} E_0^{(2)} &= 2\langle \Phi_{L/R} | \hat{h} | \Phi_{L/R} \rangle + \langle \Psi_{L/R}^d | \hat{C} | \Psi_{L/R}^d \rangle \\ &= \frac{2}{\sqrt{2}}[(1 + g^2)u - 2gw] + U \end{aligned} \quad (23)$$

for two electrons on either the left or right quantum dot—these are equivalent. The second term in this model is the

onsite interaction in the Hubbard model, U . For well-separated quantum dots, $\eta \gtrsim 1.5$, leading to $u \gg w$ and $g \ll 1$, hence $(1 + g^2) \gg 2g$. For the purposes of the following approximations, it is therefore sufficient to give onsite energy due to the momentum and potential as $\langle \Phi_{L/R} | \hat{h} | \Phi_{L/R} \rangle \approx \hbar\omega_0$ and the onsite Coulomb repulsion as $U \approx U_0$, where

$$\begin{aligned} \hbar U_0 &= \int d\mathbf{r}_1 \int d\mathbf{r}_2 [\varphi_{L/R}(\mathbf{r}_1)\varphi_{L/R}(\mathbf{r}_2) \\ &\quad \times C(\mathbf{r}_1, \mathbf{r}_2)\varphi_{L/R}(\mathbf{r}_1)\varphi_{L/R}(\mathbf{r}_2)], \end{aligned} \quad (24)$$

with $C(\mathbf{r}_1, \mathbf{r}_2) = e^2/4\pi\epsilon_r\epsilon_0|\mathbf{r}_1 - \mathbf{r}_2|$. The identity $\frac{1}{|\mathbf{r}_1 - \mathbf{r}_2|} = \frac{2}{\sqrt{\pi}} \int_0^\infty dt \exp\{-t^2(\mathbf{r}_1 - \mathbf{r}_2)^2\}$ [26] can be used to compute U_0 , giving $E_0^{(2)} \approx 2\hbar\omega_0 + c\hbar\omega_0$, where $c = (e^2/4\pi\epsilon_r\epsilon_0\tilde{a})/\hbar\omega_0$ and $\tilde{a} = \sqrt{2/\pi}a$, c being the ratio of the Coulomb energy ($e^2/4\pi\epsilon_r\epsilon_0\tilde{a}$) to the confinement energy ($\hbar\omega_0$). Overall, the charging energy is therefore $E_C \approx (1 + c)\hbar\omega_0$.

Both η and c are dependent on the confinement frequency ω_0 , as $\eta = \eta_0\omega_0$ and $c = c_0/\sqrt{\omega_0}$, where we have introduced the parameters $\eta_0 = l^2m^*/\hbar$ and $c_0 = \sqrt{\pi}m^*/2e^2/4\pi\epsilon_r\epsilon_0\hbar^{3/2}$. After increasing the confinement potential of a single electron by the charging energy, we have the new ground-state frequency $\tilde{\omega}_0 = \omega_0 + E_C/\hbar = (2 + c_0/\sqrt{\omega_0})\omega_0$, leading to a change in the ratio of barrier height to half ground-state energy, $\tilde{\eta} = (2 + c_0/\sqrt{\omega_0})\eta$. The change in barrier height is therefore dependent on the initial ground-state frequency. Typical parameters for GaAs quantum dots are $m^* = 0.067m_e$, $\epsilon_r = 12.9$, and $\hbar\omega_0 = 3$ meV [27], giving $c_0 = 5.11 \times 10^6$ Hz $^{1/2}$ and $c = c_0/\sqrt{\omega_0} = 2.39$, hence $\tilde{\omega}_0 \approx 4.39\omega_0$ and $\tilde{\eta} \approx 4.39\eta$. Thus, the energetic cost of charging is $E_C \approx 10$ meV.

The parameter regime is such that the onsite interaction is approximately $U \approx 20\Gamma$ and, since $U \approx U_0 = c\omega_0$, we find $\hbar U \approx 7.2$ meV and $\hbar\Gamma \approx 360$ μ eV, which are both plausible experimental values [20,24].

By enforcing $U = 20\Gamma$, numerically we find that $\eta = 1.86$ gives the correct ratio of onsite interaction and tunnel coupling, and therefore $\tilde{\eta} = 8.17$. The new tunnel coupling is $\tilde{\Gamma} \approx 0.0039\Gamma$. The electron hopping is therefore effectively frozen because the tunneling of a single electron would take approximately 250 times as long. If we define freezing the interactions as approximately reducing the tunnel coupling to 1% of having the interactions unfrozen, we would only require an increase in the confinement energy of approximately $0.83E_C$, see Fig. 5.

The preceding applies in the case that there are two electrons. When there is only one electron the charging energy is significantly less, as we take $c \rightarrow 0$, giving $E_C^{(1)} = \hbar\omega_0$, $\tilde{\omega}_0 = 2\omega_0$, and $\tilde{\eta} = 2\eta$. Assuming the same tunneling strength of $\hbar\Gamma = 360$ μ eV again leads to $\eta = 1.86$ and therefore the new tunneling is $\tilde{\Gamma} \approx 0.22\Gamma$, which is much greater than our definition of freezing the tunneling. In fact, in order to reach the equivalent reduction in tunneling as in the two-electron case, we must increase the confinement by about $4.5E_C \approx 13.5$ meV. Additional energy is required because with only one electron the confinement potentials are less, giving a lower central barrier due to the constant distance between the dots—see Fig. 4.

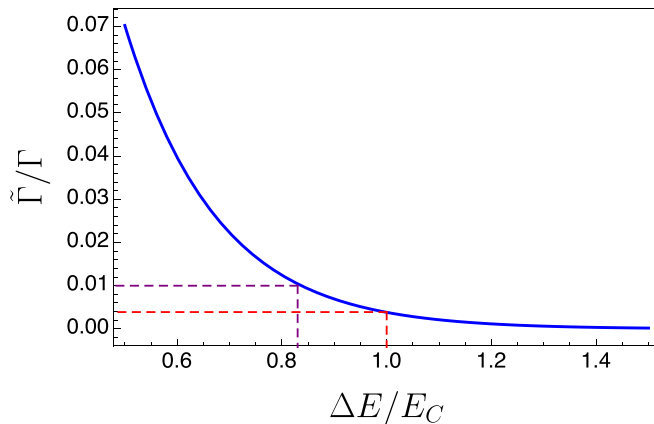


FIG. 5. The ratio of the frozen and unfrozen tunnel couplings against the energy applied, ΔE , to increase the confinement potential (the energy is given in units of the charging energy E_C). The purple dashed line shows that 1% of unfrozen tunnel coupling is achieved for $\Delta E = 0.83E_C$, and the red dashed line shows 0.4% of unfrozen tunnel coupling for $\Delta E = E_C$.

B. Shuttling

Shuttling is a proposal for transporting electrons in semiconductor devices for scalable quantum computation [14]. An early proposal involves the electron being shuttled by a surface acoustic wave [28]. Subsequent proposals have generally used arrays of quantum dots with tunable metal barrier gates to lower and raise the tunneling rate between neighboring dots, inducing a transfer of the electron through the dots sequentially [1,29–33].

For a fair comparison of the energetics, we assume the quantum dots and spacing between them for shuttling are the same as our state transfer protocol. The energetic cost of shuttling can therefore be considered the sequential loading and unloading of the quantum dots to coherently move the electrons along the chain. Although in practice this may be achieved with a separate barrier potential and raising and lowering the chemical potential of the quantum dots, in the best case this would be energetically equivalent to freezing and unfreezing the tunneling between adjacent quantum dots. The energetic cost of shuttling is therefore at least $E_{\text{shuttling}}^{(2)} = 2E_C N \approx 20N$ meV for the two-electron encoding, and $E_{\text{shuttling}}^{(1)} = E_C N \approx 13.5N$ meV for the single-electron encoding. Figure 6 shows a comparison of the energetic cost of shuttling with our perfect state transfer protocol.

C. Perfect state transfer scheme

The full energetic cost of our scheme includes freezing and unfreezing interactions but also the cost of applying the local potential ε_2 for separation and recombination of the electrons (see Fig. 3, steps 1 and 4). The local potentials applied are $\delta \gg \Gamma$; thus, as a worst case estimate, they would change the ground-state energies of the electrons by $E_\delta \approx \hbar\delta$. The total energetic cost of our protocol for two-electron encoding is therefore $E_{\text{PST}}^{(2)} = 4E_C + 2E_\delta$, independent of the length of the quantum dot chain N (more accurately, $N + 2$ due to the additional quantum dot required at each end of the chain). In

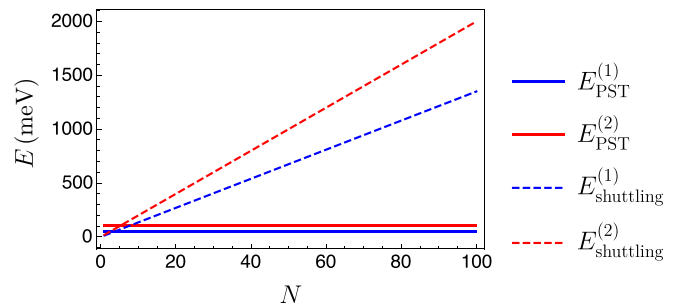


FIG. 6. Comparison of the theoretical energetic costs for the protocol with perfect state transfer (PST) and the shuttling method for logical information with both one- and two-electron encodings.

the worst case, $\delta = 40\Gamma$ and therefore $E_{\text{PST}}^{(2)} \approx 108$ meV for the two-electron logical qubit encoding.

A single-electron logical qubit encoding would only require the energetic cost of step (2) or (3) from Fig. 3. Therefore we find an energetic cost of $E_{\text{PST}}^{(1)} \approx 54$ meV, half that of the two-electron logical encoding.

D. Lower bound for classical wire

A lower bound for an interconnect in a CPU can be estimated by the energy required to charge the metal wire CV^2 , where we treat the wire as a capacitor with capacitance $C \sim \varepsilon_0 L$, with vacuum permittivity ε_0 and L the length of the wire. The minimal distinguishable voltage is $V \sim k_B T/e$ [13], where k_B is the Boltzmann constant and T is temperature, which we assume to be room temperature because we would have to consider the quantum effects of the wire in the cold regime of the quantum dots. In the cold regime we have investigated shuttling instead. The size of quantum dots with 3 meV is approximately 100 nm [27]. Hence we find the lower bound of $E_{\text{classical}} > 3.7N$ meV, where N is the equivalent number of 100-nm quantum dots for the interconnect. This bound is, of course, very conservative, and in reality, far more energy is required in current CPUs, as discussed in the Introduction. However, it is already of the same order as quantum coherent buses and, crucially, it scales with N , thus showing the advantage of the perfect state transfer protocol.

VI. NOISE

We have established the energetic advantage in the case that there is no noise. There are several sources of noise for quantum dot qubits. The most significant are nuclear spin noise and charge noise [34,35]. For tunneling electrons, another noise contribution is electron-phonon scattering [36–38]. These noise sources particularly contribute dephasing noise and lead to relatively short T_2 times compared to their relaxation times, T_1 . The coherence times depend on the qubit encoding, with charge qubits having coherence times of $T_1 = 30$ ns and $T_2 = 7$ ns [39]. For classical information as a low-dissipation classical bus, the dephasing noise only needs to be considered for maintaining coherence in the perfect state transfer part of the protocol. Given a maximum tunneling rate of $\hbar\Gamma = 360 \mu\text{eV}$, we find that the time for perfect state transfer, $T = (\pi/2)(\hbar/360 \mu\text{eV})N \approx 3N$ ps—

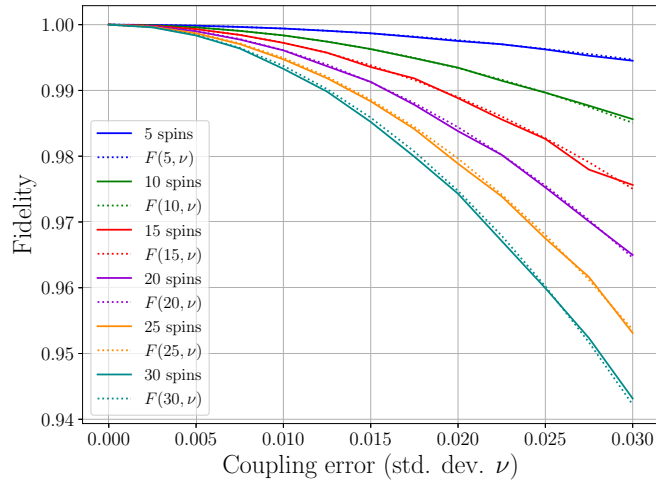


FIG. 7. Fidelity against the coupling error ν for various numbers of spins in the perfect state transfer chain. The coupling error is the standard deviation, with the maximum coupling in the chain set to 1. The numerical fit $F(n, \nu)$ is given in Eq. (25).

see Sec. III. A chain of even 300 ions would still give a transfer time significantly below the dephasing time of the charge qubits. However, the rate of voltage change required to freeze and unfreeze the chain would therefore be on the order of picoseconds, which is very fast [40]. Reducing the tunnel coupling, and therefore increasing the transfer time, can be achieved simply by increasing the confinement or increasing the distance between sites.

The main source of error would actually be the inability to tune the tunnel couplings accurately enough for perfect state transfer. Let ν be the standard deviation of the error in tuning the couplings and the largest coupling be set to 1. The tunnel couplings for perfect state transfer are $\Gamma_{i,i+1} = \sqrt{i(N-i)}$. We simulate 1000 samples of normally distributed error in the tunnel couplings for various numbers of spins. Figure 7 shows a plot of the fidelity against the error. Numerically, we find a good fit:

$$F(n, \nu) = 2 - \exp\{(0.00743n^2 + 2n - 4.29)\nu^2\}. \quad (25)$$

If the error is 1% of the maximum coupling, the number of spins must be 44 or less to achieve a fidelity of more than 0.99. Increasing the number of repetitions also increases the probability of success for a classical data bus. The probability that every one of the R repetitions fails is $(1 - F(n, \nu))^R$, so diminishes rapidly with the maximum number of repetitions.

The protocol could be applied sequentially, building up perfect state transfer chains such that the distances for each are significantly shorter than the noise that arises from mismatched tunneling rates. The energetic cost would now be dependent on N but with a very low prefactor. Even perfect state transfer chains of only ten quantum dots would provide an energetic advantage over shuttling. In the case of classical computing, we can disregard the phase information after each perfect state transfer step.

Electrons can be confined in GaAs quantum dots for long times, on the order of seconds [41]. Hence classical bit-flip errors are unlikely over the full length of the data bus. Repetition

codes can be used to improve the fidelity of bit transmission. The protocol can be performed m times, and a majority vote of the outcomes can be used to determine the state.

VII. DISCUSSION

This work considers the energetic cost of state transfer protocols in quantum dot arrays. There are two clear and separate applications for these results: Firstly, to inform the design of quantum dot arrays for quantum computing—in particular, to minimize the on-chip dissipation (heat generation), which imposes demands on the cooling power of the refrigeration; and secondly, as a proposal for the limits of what is possible for energy-efficient data buses for classical information on semiconductor chips.

The proposed perfect state transfer protocols give a theoretical energetic advantage to the current proposals of shuttling electrons. Recent work [14] on scalable quantum computing architectures in quantum dots considered the important issue of power consumption due to the control of a large number of quantum dots and the capacity to cool these devices. Low-dissipation data buses for transferring coherent quantum information would provide an avenue toward relaxing this constraint.

Quantum dots and ion-trap chains have both recently been investigated as platforms for a potential energetic advantage in performing classical computations by using qubits and the coherent evolution of quantum systems [12,42]. Here, we consider the interconnects, another important and energetically costly component of a universal computer. Using the logical encoding of Ref. [12] for semiconductor quantum dots, we find that perfect state transfer offers a significant energetic scaling advantage compared to a classical data bus. The transfer of information via coherent quantum dynamics for classical data can also reduce a source of energetic overhead for using reversible quantum devices for classical computation. Without coherent quantum interconnects, the amount of data loading and unloading from classical information could be prohibitively expensive. On the other hand, if a reasonably sized computational unit, such as an arithmetic logic unit (ALU), could be implemented with reversible quantum dynamics and quantum coherent data buses, an energetic advantage becomes more attainable.

ACKNOWLEDGMENTS

D.L. acknowledges support from the EPSRC Centre for Doctoral Training in Delivering Quantum Technologies, Grant No. Ref. EP/S021582/1. S.B. acknowledges the support of Non-Ergodic Quantum Manipulation EP/R029075/1. J.P.M. acknowledges the support of FCT - Portugal through scholarship SFRH/BD/144151/2019. Y.O. thanks the support from FCT – Fundação para a Ciência e a Tecnologia (Portugal), namely through Project No. UIDB/04540/2020, as well as from projects QuantHEP and HQCC supported by the EU QuantERA ERA-NET Cofund in Quantum Technologies and by FCT (QuantERA/0001/2019 and QuantERA/004/2021, respectively), and from the EU Quantum Flagship Project EuRyQa (101070144).

- [1] T. Fujita, T. A. Baart, C. Reichl, W. Wegscheider, and L. M. K. Vandersypen, *npj Quantum Inf.* **3**, 22 (2017).
- [2] A. M. J. Zwerfer, S. V. Amitonov, S. L. de Snoo, M. T. Madzik, M. Russ, A. Sammak, G. Scappucci, and L. M. K. Vandersypen, [arXiv:2209.00920](https://arxiv.org/abs/2209.00920).
- [3] H. Qiao, Y. P. Kandel, K. Deng, S. Fallahi, G. C. Gardner, M. J. Manfra, E. Barnes, and J. M. Nichol, *Phys. Rev. X* **10**, 031006 (2020).
- [4] S. Bose, *Phys. Rev. Lett.* **91**, 207901 (2003).
- [5] M. Christandl, N. Datta, T. C. Dorlas, A. Ekert, A. Kay, and A. J. Landahl, *Phys. Rev. A* **71**, 032312 (2005).
- [6] S. Bose, *Contemp. Phys.* **48**, 13 (2007).
- [7] R. Landauer, *IBM J. Res. Dev.* **5**, 183 (1961).
- [8] C. H. Bennett, *IBM J. Res. Dev.* **17**, 525 (1973).
- [9] E. Fredkin and T. Toffoli, *Int. J. Theor. Phys.* **21**, 219 (1982).
- [10] I. K. Hänninen, C. O. Campos-Aguillón, R. Celis-Cordova, and G. L. Snider, in *Reversible Computation*, Lecture Notes in Computer Science, edited by J. Krivine and J.-B. Stefani (Springer International Publishing, Cham, Switzerland, 2015), pp. 173–185.
- [11] C. O. Campos-Aguillón, R. Celis-Cordova, I. K. Hänninen, C. S. Lent, A. O. Orlov, and G. L. Snider, in *2016 IEEE International Conference on Rebooting Computing (ICRC)* (IEEE, New York, 2016), pp. 1–7.
- [12] J. P. Moutinho, M. Pezzutto, S. S. Pratapsi, F. F. da Silva, S. De Franceschi, S. Bose, A. T. Costa, and Y. Omar, *PRX Energy* **2**, 033002 (2023).
- [13] V. Zhirnov, R. Cavin, and L. Gammaitoni, *ICT - Energy - Concepts Towards Zero*, edited by G. Fagas, L. Gammaitoni, D. Paul, and G. A. Berini (IntechOpen, Rijeka, 2014).
- [14] J. M. Boter, J. P. Dehollain, J. P. G. van Dijk, Y. Xu, T. Hensgens, R. Versluis, H. W. Naus, J. S. Clarke, M. Veldhorst, F. Sebastiano, and L. M. K. Vandersypen, *Phys. Rev. Appl.* **18**, 024053 (2022).
- [15] T. Shi, Y. Li, Z. Song, and C.-P. Sun, *Phys. Rev. A* **71**, 032309 (2005).
- [16] M. B. Plenio and F. L. Semião, *New J. Phys.* **7**, 73 (2005).
- [17] A. Wójcik, T. Łuczak, P. Kurzyński, A. Grudka, T. Gdala, and M. Bednarska, *Phys. Rev. A* **72**, 034303 (2005).
- [18] A. Wójcik, T. Łuczak, P. Kurzyński, A. Grudka, T. Gdala, and M. Bednarska, *Phys. Rev. A* **75**, 022330 (2007).
- [19] J. Pedersen, C. Flindt, N. A. Mortensen, and A.-P. Jauho, *Phys. Rev. B* **76**, 125323 (2007).
- [20] T. Hensgens, T. Fujita, L. Janssen, X. Li, C. J. Van Diepen, C. Reichl, W. Wegscheider, S. Das Sarma, and L. M. K. Vandersypen, *Nature (London)* **548**, 70 (2017).
- [21] A. Wensauer, O. Steffens, M. Suhrke, and U. Rössler, *Phys. Rev. B* **62**, 2605 (2000).
- [22] M. Helle, A. Harju, and R. M. Nieminen, *Phys. Rev. B* **72**, 205329 (2005).
- [23] Q. Li, L. Cywiński, D. Culcer, X. Hu, and S. Das Sarma, *Phys. Rev. B* **81**, 085313 (2010).
- [24] S. Yang, X. Wang, and S. Das Sarma, *Phys. Rev. B* **83**, 161301(R) (2011).
- [25] G. Burkard, D. Loss, and D. P. DiVincenzo, *Phys. Rev. B* **59**, 2070 (1999).
- [26] K. Singer and M. V. Wilkes, *Proc. R. Soc. London A* **258**, 412 (1960).
- [27] S. M. Reimann and M. Manninen, *Rev. Mod. Phys.* **74**, 1283 (2002).
- [28] S. Hermelin, S. Takada, M. Yamamoto, S. Tarucha, A. D. Wieck, L. Saminadayar, C. Bäuerle, and T. Meunier, *Nature (London)* **477**, 435 (2011).
- [29] T. A. Baart, M. Shafiei, T. Fujita, C. Reichl, W. Wegscheider, and L. M. K. Vandersypen, *Nat. Nanotechnol.* **11**, 330 (2016).
- [30] A. R. Mills, D. M. Zajac, M. J. Gullans, F. J. Schupp, T. M. Hazard, and J. R. Petta, *Nat. Commun.* **10**, 1063 (2019).
- [31] B. Buonacorsi, B. Shaw, and J. Baugh, *Phys. Rev. B* **102**, 125406 (2020).
- [32] F. Ginzel, A. R. Mills, J. R. Petta, and G. Burkard, *Phys. Rev. B* **102**, 195418 (2020).
- [33] I. Seidler, T. Struck, R. Xue, N. Focke, S. Trellenkamp, H. Bluhm, and L. R. Schreiber, *npj Quantum Information* **8**, 100 (2022).
- [34] A. V. Kuhlmann, J. Houel, A. Ludwig, L. Greuter, D. Reuter, A. D. Wieck, M. Poggio, and R. J. Warburton, *Nat. Phys.* **9**, 570 (2013).
- [35] D. Fernández-Fernández, Y. Ban, and G. Platero, *Phys. Rev. Appl.* **18**, 054090 (2022).
- [36] X. Hu, *Phys. Rev. B* **83**, 165322 (2011).
- [37] V. Kornich, C. Kloeffer, and D. Loss, *Phys. Rev. B* **89**, 085410 (2014).
- [38] G. He, G. X. Chan, and X. Wang, *Adv. Quantum Technol.*, **6**, 2200074 (2023).
- [39] A. Chatterjee, P. Stevenson, S. De Franceschi, A. Morello, N. P. de Leon, and F. Kuemmeth, *Nat. Rev. Phys.* **3**, 157 (2021).
- [40] L. Zou, S. Gupta, and C. Caloz, *IEEE Microwave Wireless Compon. Lett.* **27**, 467 (2017).
- [41] L. C. Camenzind, L. Yu, P. Stano, J. D. Zimmerman, A. C. Gossard, D. Loss, and D. M. Zumbühl, *Nat. Commun.* **9**, 3454 (2018).
- [42] S. S. Pratapsi, P. H. Huber, P. Barthel, S. Bose, C. Wunderlich, and Y. Omar, [arXiv:2210.10470](https://arxiv.org/abs/2210.10470).